P-11-38

The Greenland Analogue Project

Geomodel version 1 of the Kangerlussuaq area on Western Greenland

Jon Engström, Geological Survey of Finland

Markku Paananen, Geological Survey of Finland

Knud Erik Klint, The National Geological Survey of Denmark and Greenland

February 2012

Svensk Kärnbränslehantering AB
Swedish Nuclear Fuel
and Waste Management Co

Box 250, SE-101 24 Stockholm
Phone +46 8 459 84 00

ISSN 1651-4416
SKB P-11-38

The Greenland Analogue Project

Geomodel version 1 of the Kangerlussuaq area on Western Greenland

Jon Engström, Geological Survey of Finland

Markku Paananen, Geological Survey of Finland

Knud Erik Klint, The National Geological Survey of Denmark and Greenland

February 2012

Keywords: Greenland Analogue Project, Geomodel version 1, Kangerlussuaq area, West Greenland, Deformation zones/Faults.

Abstract

During the 2nd annual Greenland Analogue Project modelling workshop in Toronto, November 2010, the hydrological modellers requested an updated geological map and structural model of the field area around Kangerlussuaq, Western Greenland. This report presents an updated GAP geomodel which utilizes all available information in order to improve the accuracy of the model, especially beneath the ice sheet.

The modelling area was divided into two scales: The regional scale area and the site scale area. The site scale refers to the area were surface mapping has been performed, and where two boreholes (DH-GAP01 and DH-GAP03) were drilled during 2009. Geological and topographical maps from GEUS (sub-model 1) and data extracted from the geophysical map, GEUS, (sub-model 2) were used in the process to develop GAP geomodel version 1. These two interpretations were independent from each other and in the final stage these sub-models were integrated and developed into GAP geological model version 1. The integration resulted in a total of 158 lineaments. These lineaments are referred in the final model as deformation zones and faults, where deformation zones are larger features and faults are single fractures indicating some sense of movement. Four different sets of deformation zones and faults were identified in the regional area. The most prominent feature is the ductile/brittle roughly ENE-WSW trending zones crosscutting the whole area, referred as Type 1. Type 2 and Type 3 zones are in general smaller scale than Type 1 and mostly dominated by brittle deformation. The Type 2 system generally trends NW-SE, while the Type 3 system generally trends NE-SW. The Type 4 features are a brittle and roughly N-S orientated younger system, thus crosscutting all other types.

Confirmation and validation of the regional model is based on detailed surface-based examination of fractures within the site area, although the scale is different the same orientations were also identified in the regional lineament interpretation. The site area lineament model is coupled with major tectonic events in Western Greenland to further improve the certainty of our interpretation.

This report describes solely a structural 2-D model and the data produced in this report were developed into a 3-D model that together with hydrological properties serves as basis for the future hydrological modelling within the GAP project, however this work is described in a separate report (Follin et al. 2011).

Sammanfattning

I samband med den årliga GAP workshopen i Toronto i November 2010, begärde de hydrologiska modellörerna en uppdaterad geologisk och deformationszons modell i området runt omkring Kangerlussuaq, Västra Grönland. Denna rapport beskriver framtagandet av en uppdaterad GAP geomodell, vilken använder all tillgänglig information som finns, speciellt i syfte att förbättra modellen i de istäckta områdena.

Modelleringsområdet delades in i två delområden det regionala området och vårt platsundersökningsområde. Geologisk och topografisk data från GEUS (sub-modell 1) samt data extraherat från GEUS geofysik karta (sub-modell 2) användes för att producera två olika sub-modeller. Dessa två modeller producerades skilt för sig och integrerades sedan till den slutgiltiga GAP geologiska modellen version 1. Denna modell innehöll 158 lineament och i den slutgiltiga versionen refereras lineamenten som deformationszoner och förkastningar, där deformationszonerna är större spröda och plastiska zoner medan däremot förkastningarna är en spricka som uppvisar nån form av rörelse. Modellen uppvisar fyra olika typer av deformationszoner och förkastningar i det regionala området. De tydligaste zonerna är de spröda-plastiska Typ 1-zonerna som går igenom hela vårt regionala område i en ungefärlig öst-västlig riktning. Typ 2- och Typ 3-zonerna är för det mesta mindre zoner än Typ 1-zonerna och kännetecknas av att vara spröda. Typ 2-zonerna har sydostlig-nordvästlig riktning medan Typ 3-zonerna är av sydvästlig-nordostlig riktning. De yngsta zonerna är främst förkastningar och de har en nord-sydlig riktning och definieras i modellen som Typ 4.

Den regionala modellen jämfördes sedan med sprickdata från vårt forskningsområde och liknande zoner samt förkastningar kunde även hittas där. Till sist gjordes en koppling mellan den tektoniska historien i vårt forskningsområde och den i Västra Grönland. Materialet från denna modell har sedan vidareutvecklats till en 3D-modell som tillsammans med den hydrologiska datan ligger som grund för den fortsatta hydrologiska modelleringen inom GAP-projektet, men detta arbete beskrivs i en separat rapport (Follin et al. 2011).

Contents

1 Introduction

During the 2nd annual GAP modelling workshop in Toronto, November 2010, the hydrological modellers requested an updated geological map and deformation zone model of the field area around Kangerlussuaq, Western Greenland. In the workshop it was concluded the previous model was insufficient to meet the demands of hydraulic modelling, this was mainly that due to the very simplistic and stochastic nature of the previous model, which was based on superficial interpretation of site scale lineaments and the mapping data collected from small key areas in 2008 (Aaltonen et al. 2010). The target area of the full-scale hydrogeological modelling is very large compared to the field area of the sub-project C (SPC) and a significant part of it is covered by ice. In order to response to the modellers request so that the updating could rest on sound argumentation, a sub-model area about 70 km by 110 km was defined so that it was mainly in the ice free region. In the east, the sub-model area is restricted by the availability of the airborne geophysical data to about 40 km east of the ice-margin (Figure 1-1).

The model in this report is a lineament model constructed as an interpretation from GEUS ArcGIS data, with topographical, geological and geophysical data acquired from the updated GEUS map over Western Greenland (Garde and Marker 2010). The report includes a suggested connection to the regional tectonic history and also a possible simple stress history, however due to limited amount of collected site information these should be referred as a tentative analysis

This report describes solely a structural 2-D model and the data produced in this report were developed into a 3-D model that together with hydrological properties serves as basis for the future hydrological modelling within the GAP project, however this work is described in a separate report (Follin et al. 2011).

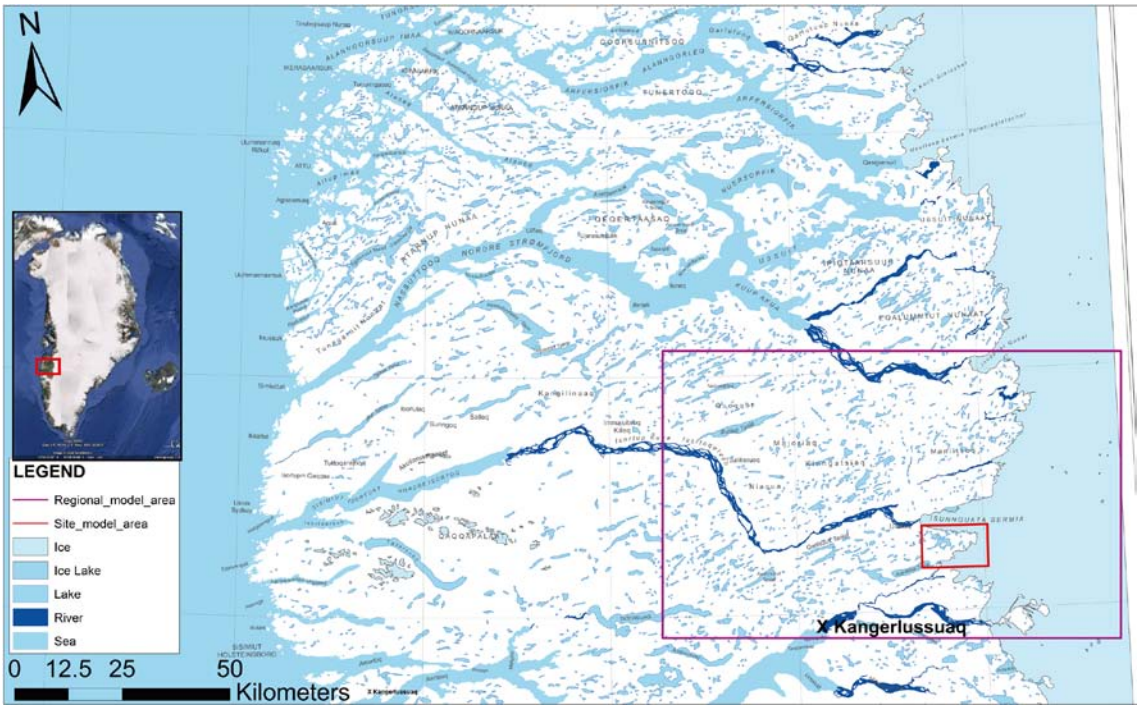

Figure 1-1. *General overview over GAP modelling area. The GAP geomodel area is shown in lilac (larger box) and the site scale area in red (smaller box). The map is modified from GEUS (Geological Survey of Denmark and Greenland) Geological map 2010 (Garde and Marker 2010).*

2 Objective and scope

The updated GAP geomodel utilizes all available information in order to improve the accuracy of the model, especially beneath the ice sheet. The aim of the geomodelling work was to start with the large scale features and then work towards more detailed scales. Special attention is directed towards the identification of lineaments that constitutes potentially brittle structures, which may outline hydraulic conductive zones. The modelling area was divided into two scales the regional scale area and the site scale area (Figure 2-1). The site scale refers to the area were surface mapping has been performed in 2008 (Aaltonen et al. 2010), and where DH-GAP01 and DH-GAP03 were drilled during 2009 (SKB 2010). This separation into two different scales is done so that a more detailed examination and interpretation of the site scale area can be conducted in the future when more detailed data is gathered.

The coordinates of the modelling area (regional area, lilac rectangle in Figure 2-1) are:
NW corner: 214504; 7508404
NE corner: 319746; 7495482
SW corner: 206444; 7442218
SE corner: 311563; 7429378

These coordinates are in the Projected Coordinate System NAD 1983 Complex UTM Zone 23N, for which the GEUS geological map applies. However, the GAP project database is in the Projected Coordinate System WGS 1984 Complex UTM Zone 22N.

The coordinates in this system of the regional modelling area are:
NW corner: 469885; 7493368
NE corner: 576217; 7490673
SW corner: 468187; 7426678
SE corner: 574508; 7423937

The GAP site area (the smaller red rectangle in Figure 2-1) has the following coordinates:
NW corner: 528881; 7451274
NE corner: 544208; 7451274
SW corner: 528881; 7441489
SE corner: 544208; 7441489

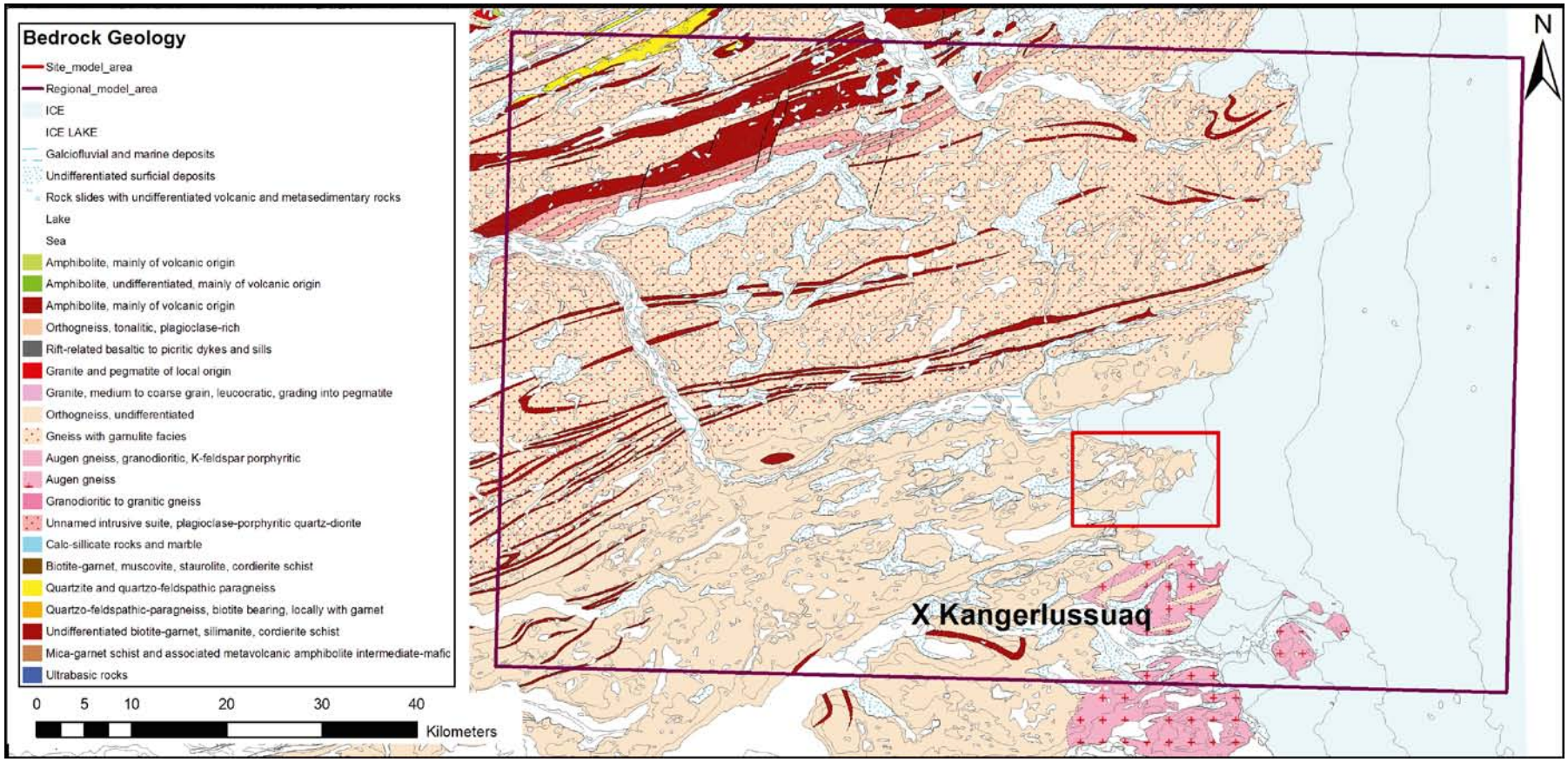

Figure 2-1. *Map showing the regional modelling area for the GAP geomodel in lilac and the site scale area in red. Geology is adapted from GEUS Geological map (Garde and Marker 2010).*

3 Description of maps, data and software used during the development of the GAP geomodel

Geological and topographical maps from GEUS (sub-model 1) and data extracted from the geophysical map, GEUS, (sub-model 2) were used in the process to develop the final GAP geomodel. These two interpretations were undertaken independently. The geophysical lineament interpretation (sub-model 2) was done on aeromagnetic data to confirm and validate sub-model 1, the two sub-models where then integrated and developed into GAP geological model version 1.

3.1 Description of maps used during the development of sub-model 1; geological/topographical interpretation

GEUS recently published (Garde and Marker 2010) an updated geological map over West Greenland; which is an update of the work by Escher (1971). Together with the geological information from this map and the topography in the area, a lineament interpretation was performed for the regional area outlined in Figure 2-1.

3.2 Description of data and software used during the development of the sub-model 2; geophysical interpretation

In order to study the occurrence of brittle deformation within the study area, interpretation of magnetic lineaments from the aeromagnetic data was carried out. This study was done totally independent from sub-model 1 and the outcome from it was defined as sub-model 2.

The data were acquired from GEUS and it was extracted from aeromagnetic data that GEUS reported in 2004 (Jensen et al. 2004). Magnetic lineaments are linear, continuous features on a magnetic map possibly related to deformation zones or rock type contacts. In general, the magnetic properties of a deformation zone may vary depending on its geological history in the following ways (McIntyre 1980, Henkel and Guzmán 1977, Johnson and Merril 1972):

- Oxidizing fluid intrudes into the rock material during the metamorphism: deposition of magnetite; magnetic susceptibility increases.
- Reducing metamorphic fluid intrudes into the rock material: magnetite is transformed to non-magnetic hematite; susceptibility decreases.
- Low temperature (< 250°C) weathering in a fracture zone: magnetite is decomposed; susceptibility decreases.

According to these options, a deformation zone may induce a magnetic minimum or maximum. Brittle zones commonly carry water, allowing different chemical and physical weathering processes to take place within the zone, resulting in decomposition of magnetite to hematite. Since low-temperature weathering is supposedly the most recent chemical process in the brittle zones, it is therefore justified to assume that most linear magnetic minima represent their surface expressions. Also a sharp discontinuity or a displacement of magnetic anomalies may be an indication of a potential brittle deformation zone.

For the lineament interpretation, the GEUS geophysical airborne data (Jensen et al. 2004) was further processed using Geosoft Oasis software, and the following series of maps was created:

- Magnetic total field, colour-shaded and grey-shaded map (shading from 0°, 45°, 90° and 135°).
- Vertical derivative of magnetic total field, colour-shaded and grey-shaded map.
- Horizontal derivative of magnetic total field, colour-shaded and grey-shaded map.
- Analytic signal, colour-shaded map.
- Tilt derivative of magnetic total field and its horizontal derivative, colour-shaded map.
- Theta derivative (absolute value of tilt derivative), colour-shaded map.
- TDX derivative (complement angle of tilt derivative), colour-shaded map.

4 Execution of the GAP geomodel

4.1 General

The work on updating the regional model started in January 2011, although some work on the site scale model and some general outlines for the regional model were already initiated in 2010. This work included processing of mapping data that the GAP project collected during 2008–2010 and the analysis of fracture data from the pilot holes (DH-GAP01 and DH-GAP03) drilled in 2009. In addition, a regional lineament map was produced by integrating geological information and the topographical indications; sub-model 1, while a magnetic lineament map was produced from the aeromagnetic data as an independent study, thus defined as sub-model 2. Combination of these sub-models 1 and 2 comprise the GAP geological model version 1. The result was validated against mapping and drillhole data in the site area and a connection to the tectonic history was tentatively suggested by reviewing literature and examination of the limited amount of mapping data.

4.2 Sub-model 1; Lineament interpretation from geological and topographical data

The geologic and the topographic maps of the regional area were examined and formed the basis for the lineament interpretation in sub-model 1. From these maps 104 lineaments were interpreted (Figure 4-1). The most prominent features are the roughly ENE-WSW trending Type 1 (lilac) lineaments that crosscut the entire area. The Type 2 (green) and the Type 3 (blue) lineaments are in general a smaller scale system than the Type 1. The Type 2 system generally trend NW-SE, while the Type 3 system generally trends NE-SW. The Type 4 (black) is an N-S system that crosscuts all other types, therefore it is younger.

4.3 Sub-model 2; Geophysical lineament interpretation from GEUS data

The standard maps utilized in the interpretation comprise magnetic total field, horizontal, vertical and total gradient (analytic signal) and different normalized magnetic derivatives (tilt, theta and TDX derivative). The suitability of normalized gradients in structural mapping is well known, and their interpretational meaning is discussed in e.g. Fairhead and Williams (2006), Fairhead et al. (2007), and Salem et al. (2008). Their main advantage is that they help normalize the signatures in images of magnetic data so that weak, small amplitude anomalies can be amplified relative to stronger ones. Figures 4-2 to 4-5 show some examples of the compiled maps used in the interpretation. In addition to the standard maps, a grid curvature analysis (Phillips 2007) was done, revealing the locations of local and continuous magnetic minima (Figure 4-6). Data processing and map compilations were done by using Geosoft Oasis software.

The interpretation was carried out by visually inspecting the different geophysical maps in ArcGIS and by digitizing the geometry of each interpreted lineament. The lineaments were collated into a single ArcGIS theme, accompanied by an attribute table (Appendix 1) that includes the identifier and a reference to the data for each interpreted feature.

The number of interpreted lineaments shown in Figure 4-7 is 133. Their main trend is ENE-WSW (Type 1) with a clear cross-cutting trend NNE-SSW (Type 4). Other less distinct trends are NW-SE (Type 2) and NE-SW (Type 3). A number of lineaments could also be followed to the eastern part of the studied area covered by the ice sheet. In Figure 4-8, a statistical trend distribution of the lineaments is presented, showing the significance of the main trend ENE-WSW.

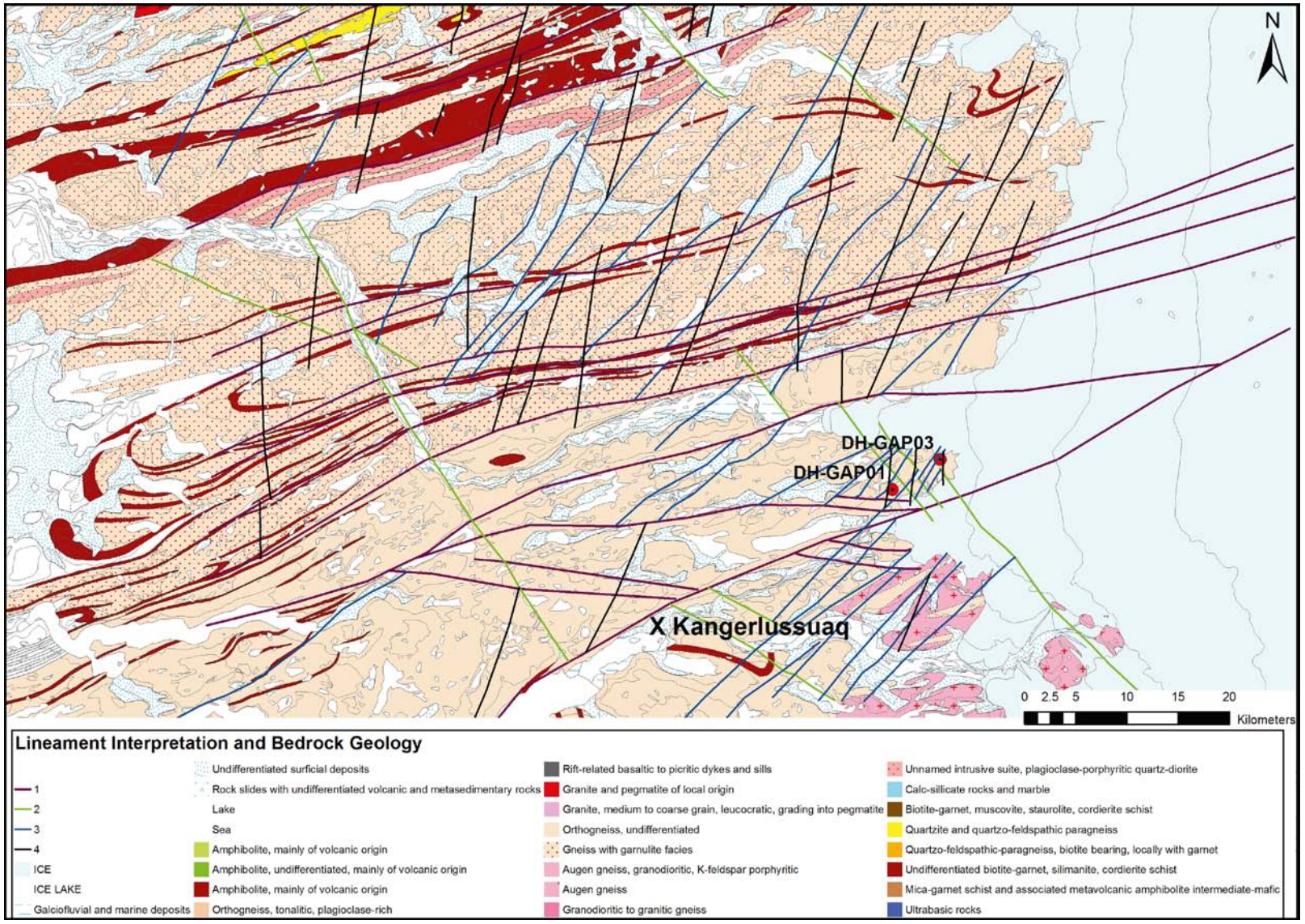

Figure 4-1. *Map showing the lineaments/deformation zones in the regional area, interpreted from geological and topographical data. The different line colours refer to different Types of lineaments/deformation zones. Geology is adapted from GEUS geological map (Garde and Marker 2010).*

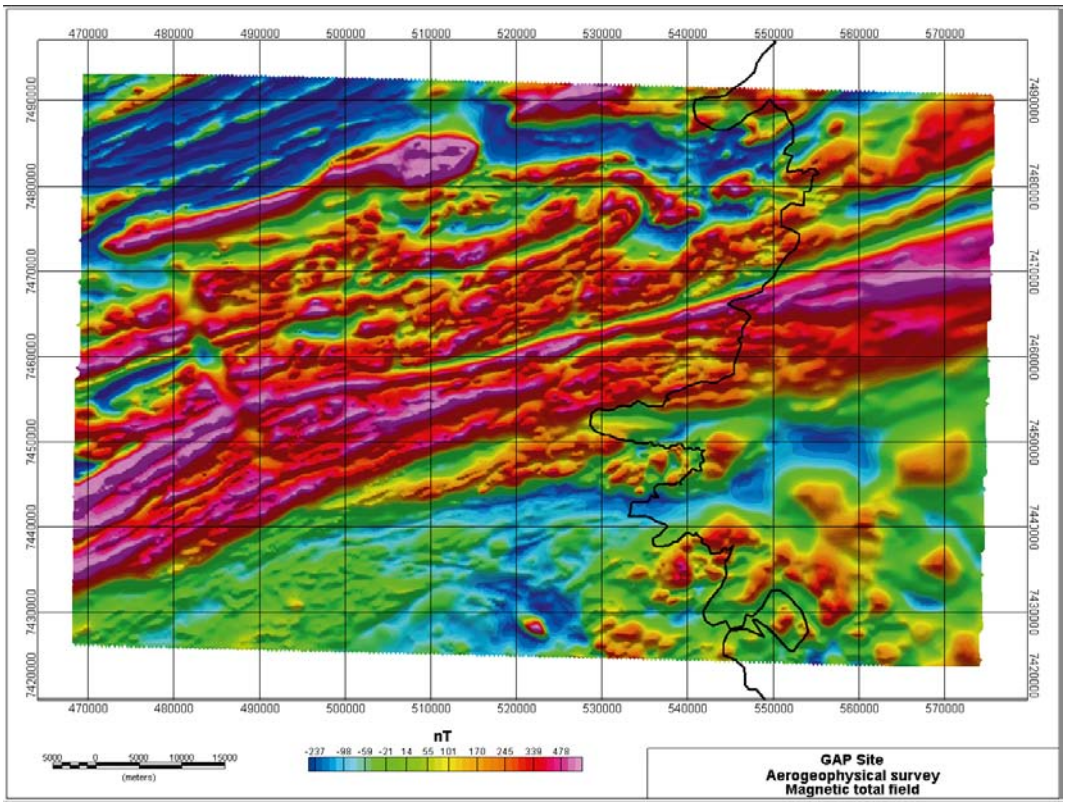

Figure 4-2. *Geophysical map showing the magnetic total field. The black line indicates the ice-margin.*

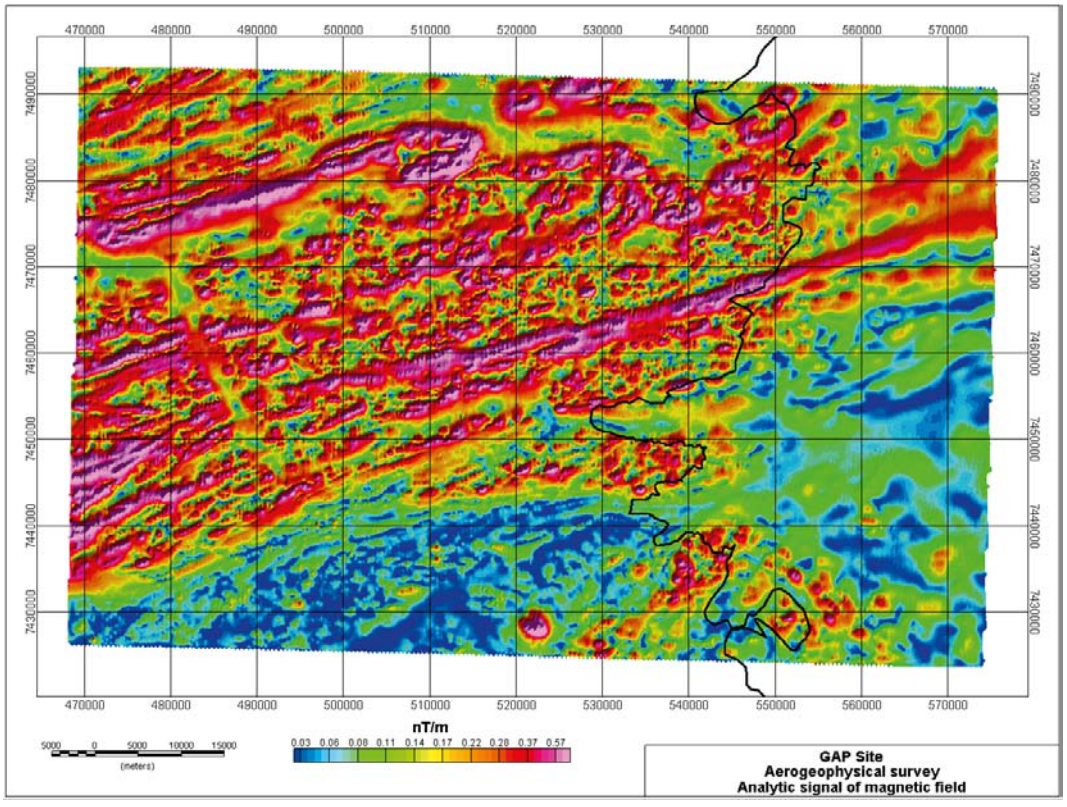

Figure 4-3. *Geophysical map showing the analytic signal (total gradient) of magnetic field. The black line indicates the ice-margin.*

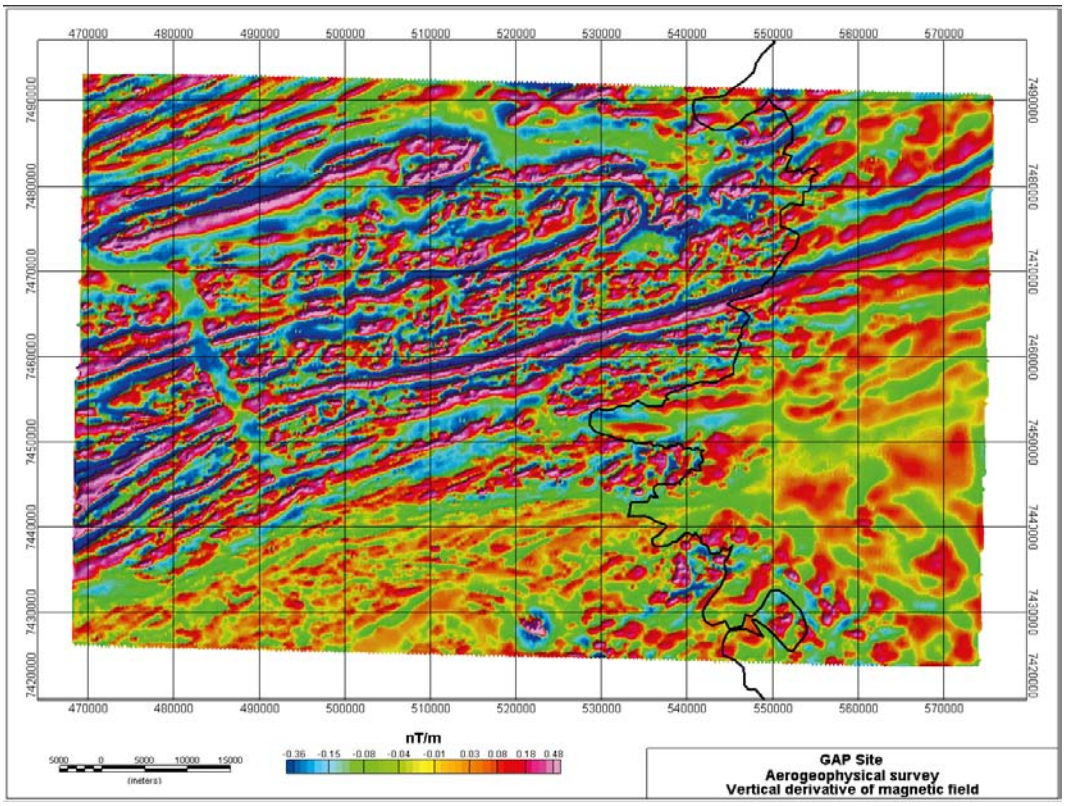

Figure 4-4. *Geophysical map showing the vertical derivative of magnetic field. The black line indicates the ice-margin.*

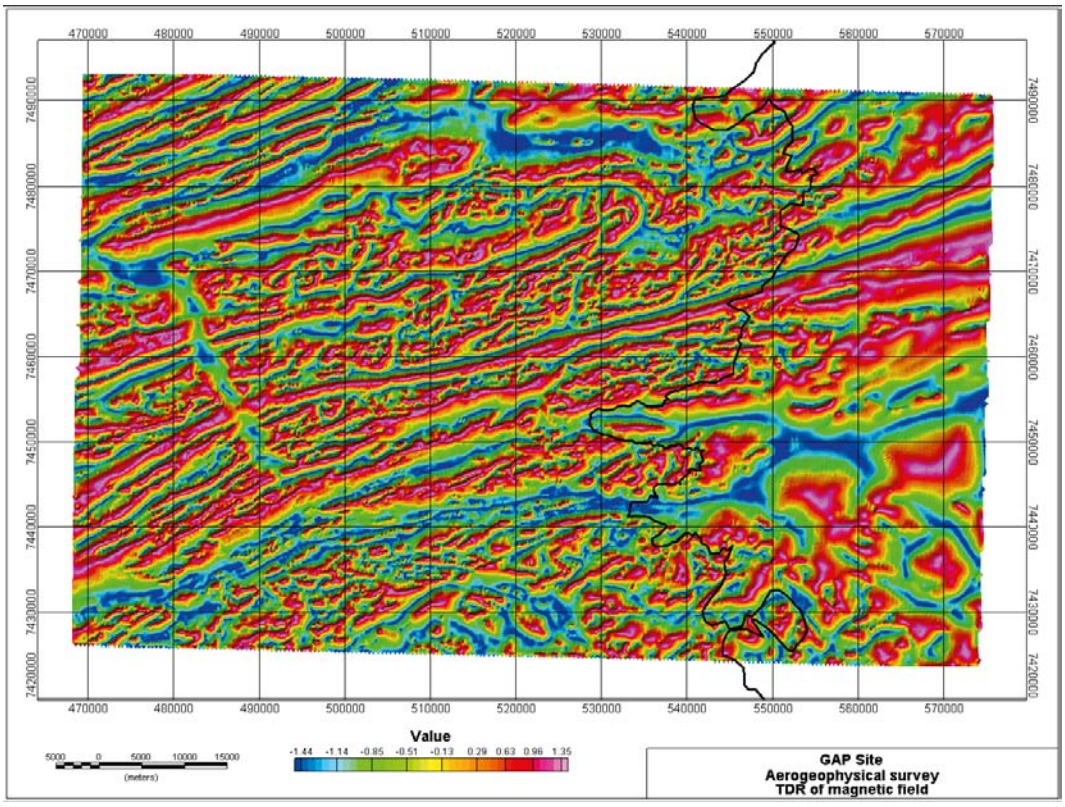

Figure 4-5. *Geophysical map showing the tilt derivative of magnetic field. The black line indicates the ice-margin.*

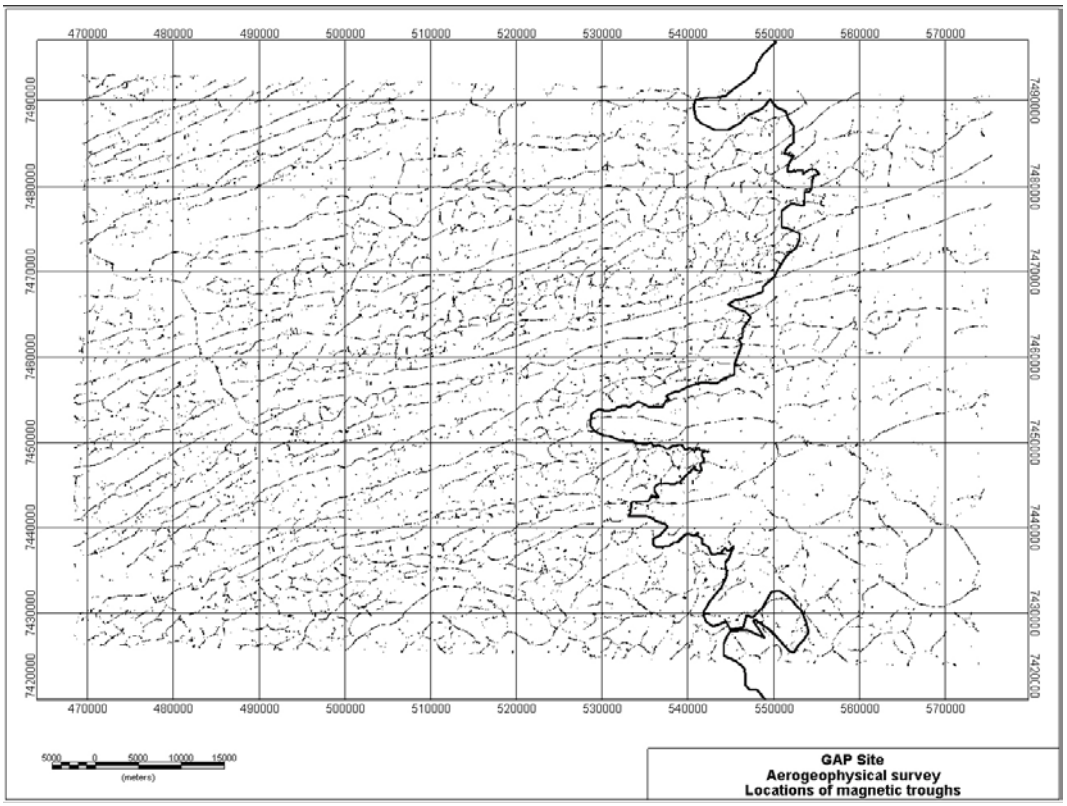

Figure 4-6. *Geophysical map showing the locations of local magnetic minima (troughs) from grid curvature analysis. The thick black line indicates the ice-margin.*

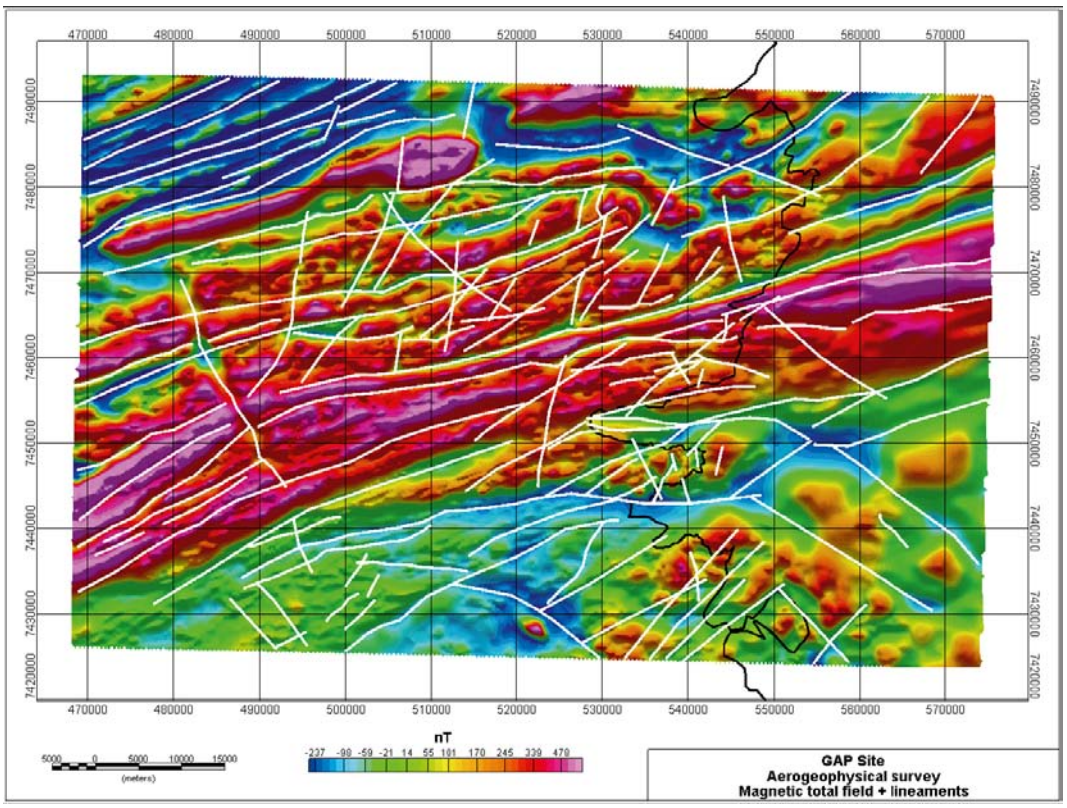

Figure 4-7. *Geophysical map showing all interpreted lineaments in (white colour) on magnetic total field map. The black line indicates the ice-margin.*

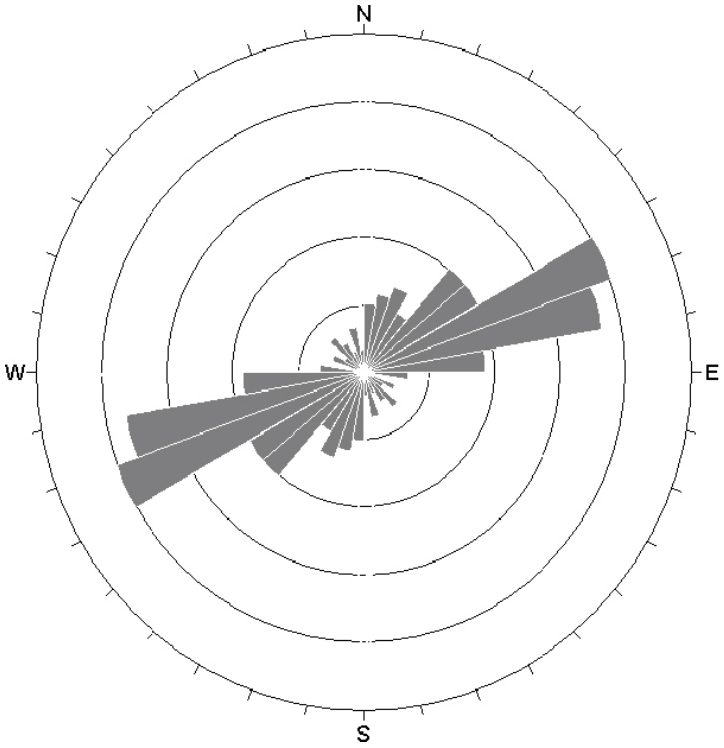

Figure 4-8. *Rose diagram showing the strikes of the interpreted geophysical lineaments (n = 133).*

4.4 Combining the two separate sub-models into the final deformation zone model

As could be expected, the two separate lineament interpretations produced different results so a joint interpretation of the two sub-models was carried out. This is illustrated in Figure 4-9, where it is evident that some modifications to the initial interpretations had to be performed. This was done by modifying the sub-model 1 lineaments to follow the lineaments from the geophysical interpretation. Also a number of new lineaments were added to the final model based on the geophysical lineament interpretation. The joint interpretation of Sub-model 1 and Sub-model 2 were merged into a final interpretation and the final model; GAP geological model version 1.

The integration of the two sub-models into one resulted in a total of 158 lineaments. These lineaments are referred in the GAP geological model version 1 as deformation zones and faults (Figure 4-10). Even though this model is merely a lineament model constructed as an interpretation from GEUS ArcGIS data, lineaments were named as deformation zones and faults. The basic assumption is that these lineaments are the intersection of deformation zones at the surface, and thus named so in the final model. In the site area we have also confirmed the existence of a few of these deformation zones but it is important to keep in mind that this is a very limited area compared to the whole regional scale modelling area.

The number of deformation zones/faults identified in both sub-models was 54, while 53 zones were solely interpreted from the geological/topographical data and 51 zones were exclusively identified in the geophysical interpretation. Both sub-models include zones of all four types, but the geological/topographical model includes more Type 4 zones and the geophysical model contains more Type 1 zones. Out of the 158 deformation zones/faults 18 occur within the site scale area shown in Figure 2-1 and 7 of these were also identified during field mapping.

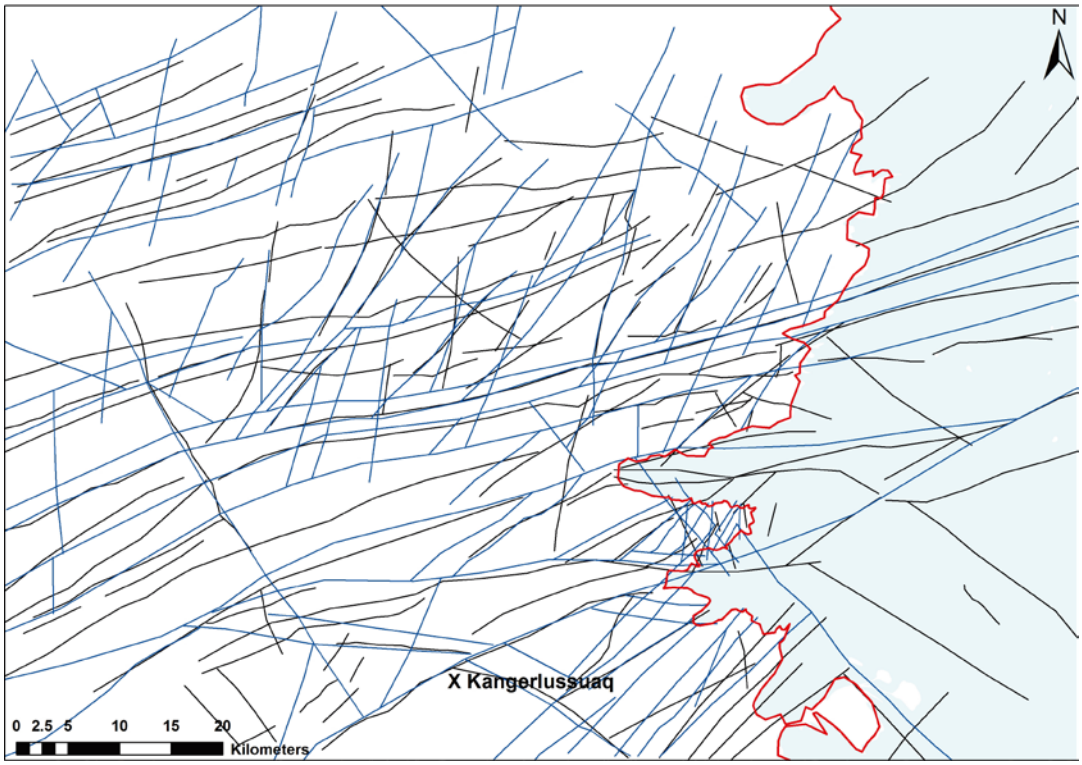

Figure 4-9. *Map including interpretation from both sub-models of the regional area. The geophysical lineaments (Sub-model 2) are illustrated with black colour and the geological/topographical lineaments (Sub-model 1) with blue colour. The red line represents the ice-margin and the ice sheet is illustrated with shaded pale blue.*

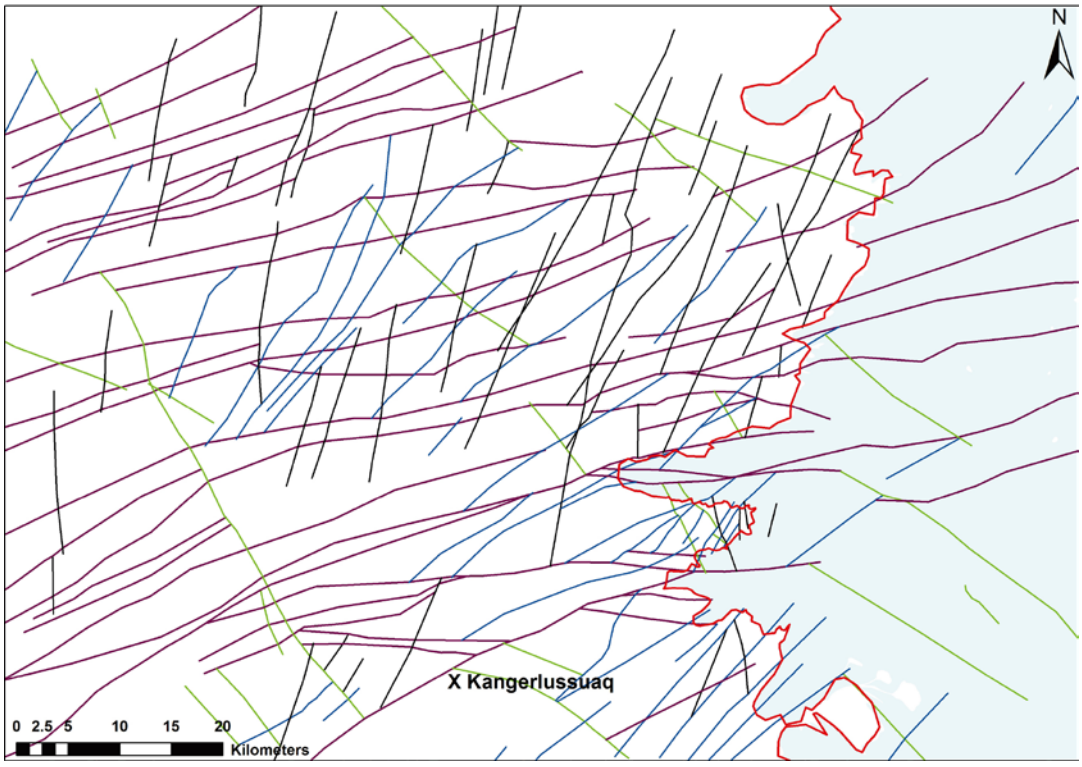

Figure 4-10. *Map showing the final interpretation of the regional area with the four different types of deformation zones and faults; Type 1=Lilac, Type 2=Green, Type 3=Blue and Type 4=Black. The red line represents the ice-margin and the ice sheet is illustrated with pale blue.*

4.5 Processing the collected GAP mapping data

To confirm and validate our regional model, a comparison to our site area was performed. The mapping data from all three years of fieldwork (2008–2010) were compiled into one file to get a comprehensive understanding of the geological features in our site area. Special emphasis was put on the assessment of faults and slickensided fracture planes to compare them to regional scale features. This was done by comparing the orientation from the lineament interpretation and the orientation from the mapping data. This procedure is evidently very basic and therefore now certain conclusions can be drawn from this interpretation. In Figure 4-11 all slickenside fractures from our site area is plotted in a stereographic plot with a Fisher contouring.

From the mapping data four different sets of faults are recognized defined by the orientation (Figure 4-12). Even though this interpretation is rugged and solely done by comparing orientation, the same sets of orientation are identified in both the lineament interpretation and the mapping data. These four different fault sets utilises the same colour code as in the regional model; for Type 1 Lilac, for Type 2 Green, for Type 3 Blue and for Type 4 Black (Figure 4-12). In addition to these four sets, a fifth set is distinguishable from the slickenside fractures showing a sub-horizontal dip, this set was given a red colour and is referred to as Type 5. Sub-horizontal fractures and faults are not readily observed in outcrops and, hence they are undervalued in mapping data. Virtually all our observations (for Type 5 fractures) are coming from the two drillcores; therefore, it is not actually known how widespread this set is in the study area. However, based on the experience from Finland and Sweden, it is known that they are common and that they have an important role in water conductivity in the upper 200 m or so e.g. Olofsson et al. (2007); Löfman et al. (2009).

The most distinct fault set in the stereographic plot is the E-W (ID=1) trending sub-vertical feature (Type 1), which shows a sub-vertical dip towards N. Type 2 faults dip either to NE (ID=2) or to SW (ID=7). Dip to NE dominate (75%) over the SW direction (25%). Type 3 faults have a more diverse character, exhibiting moderate dips towards SE (ID=3) and NW (ID=6), statistically in equal frequency. A simplification to the model is these Type 2 faults and Type 3 faults which are classified as dipping towards each other. This interpretation is done based on a few field observations; hence the evidence for these orientational sets is limited. Type 4 feature trends NNE-SSW (ID=4) showing a sub-vertical dip both towards E and W. As mentioned before, Type 5 faults are indentified only from drill cores DH-GAP01 and DH-GAP03. Dip of these fractures seem to be towards SE (ID=5), but the small number of measurements leaves uncertainty to the interpretation, this set is therefore excluded from the final model.

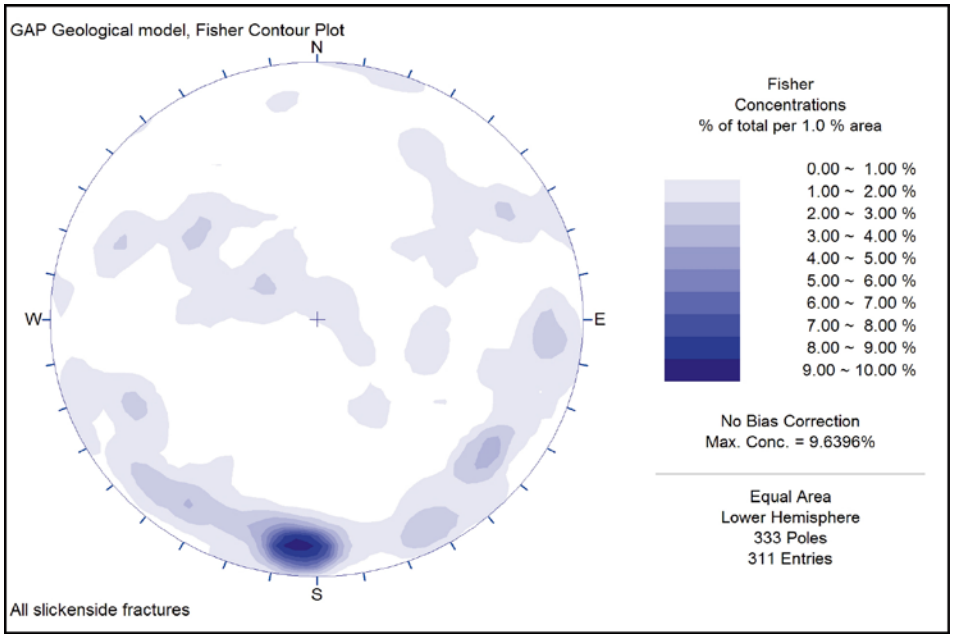

Figure 4-11. *Fisher concentrations as a contoured stereographic plot showing all measured fractures with slickenside surface. Equal area, lower hemisphere projection.*

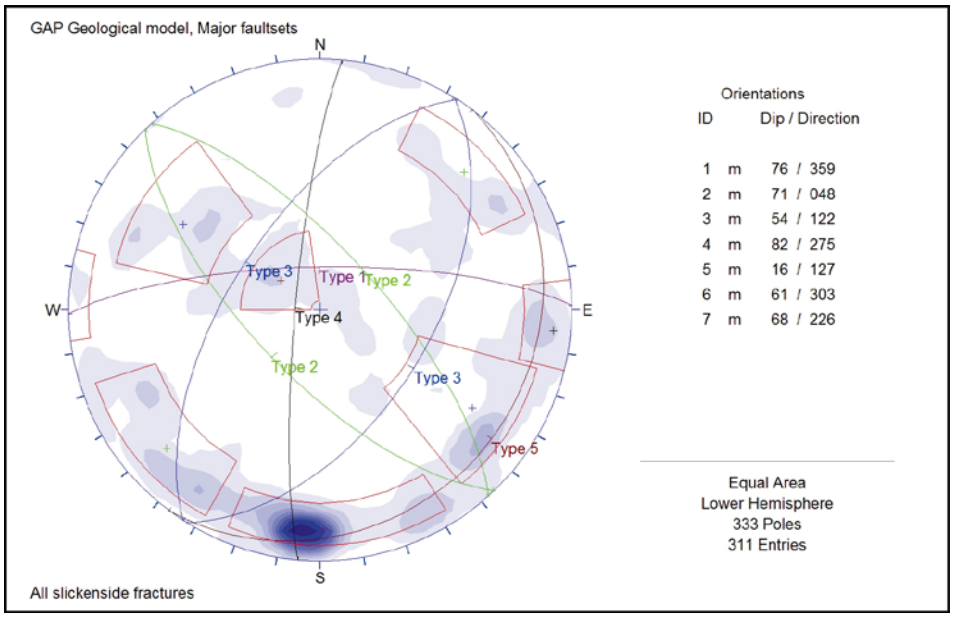

Figure 4-12. *Stereographic plot of the major fault sets interpreted from the slickenside fractures mapped by GAP from the site area. The measurements together with the interpreted plane are shown in the stereographic plot. Type 1 lilac, Type 2 green, Type 3 blue, Type 4 black and Type 5 red.*

4.6 Tentative tectonic history and related stress fields in the Kangerlussuaq area

Generally the stress conditions in Greenland are very poorly known compared to the rest of the world and there is no measurement of the stress conditions within the site area. The tectonic history of the area may be solved to some extent, but the sum of the present stress conditions prevailing in the basement remains speculative. However, some indications on the stress history may be deduced from the tectonic history of western Greenland. The tectonic history in the site area is coupled together with major tectonic events in western Greenland. Some of the structures in the GAP site area are still not validated, so additional fieldwork for a final updated event stratigraphic model is required.

Our field evidence from the site area is in good accordance with other studies conducted in Western Greenland e.g. Wilson et al. (2006). The first notable stage of deformation is ductile deformation producing open big scale folds, followed by the formation of large shear zones with semi-ductile character and dextral sense of shear. This folding is observed in the vicinity of DH-GAP03, while the semi-ductile shear zones are observed in an E-W direction south of DH-GAP01 (Figure 4-1). The dextral sense of shear for these semi-ductile shear zones is clearly illustrated in Figure 4-13, and the brittle deformation is exemplified in Figure 4-14. Based on acquired field evidence and literature studies e.g. Wilson et al. (2006) a tentative tectonic history of the study area is outlined below (Table 4-1, Figures 4-15 and 4-16).

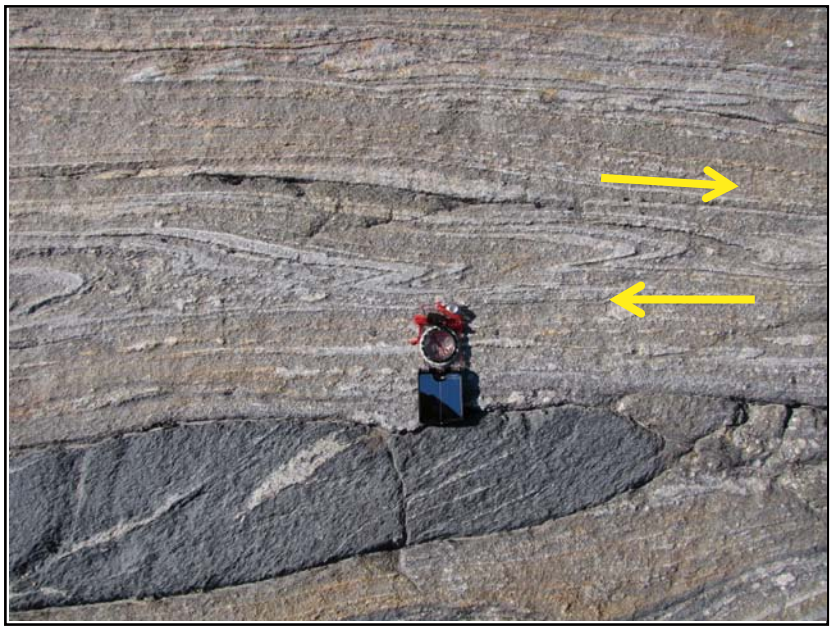

Figure 4-13. *An E-W orientated semi-ductile shear zone with dextral sense of shear (Type 1), photo taken south of DH-GAP01. Photo by Jon Engström.*

Figure 4-14. *Evidence for brittle deformation showing thrust faulting (Type 2), photo taken from a fault located between DH-GAP01 and DH-GAP03. Photo by Knud Erik Klint.*

Table 4-1. Tectonic History of the Kangerlussuaq area, adapted from Wilson et al. (2006).

Age	Description of tectonic event	Connection to geomodel	Pairing to figures
> 2.5 Ga (Archean)	Formation of banded gneiss.		
ca. 2.04 Ga	Continental rifting coupled with mafic dyke intrusions (Kangaamiut mafic dyke).		Bullet 1 in Figure 4-13 and Bullet 1 in 4-14
1.92–1.87 Ga	Continental collision. Reworking and folding of gneiss/mafic rocks.		Bullet 3 in Figure 4-13 and Bullet 2 in 4-14
1.87–1.84 Ga	Peak metamorphism, pegmatite intrusions, large scale folding/tilting.		Bullet 4 in Figure 4-13 and Bullet 2 in 4-14
1.84–1.82 Ga	Formation of shearzones, foliation parallel, E-W with a semi-ductile dextral shear and thrust faulting.	**Type 1** and **3** deformation zones/faults, **Lilac** and **Blue** system.	Bullet 5 in Figure 4-13 and Bullet 3 in 4-14
1.82–1.78 Ga	Collision and rotation of max stress direction, roughly NW-SE trending sinistral shears and conjugating thrust faulting.	**Type 2** faults, **Green** system.	Bullet 6 in Figure 4-13 and Bullet 4 in 4-14
Ca. 1.78 to present day	Various stress conditions and formation/reactivation of open mode fractures at more shallow depths during the 20–25 km uplift.		
1.2 Ga	Diamond-bearing ultramafic lamprophyres intrusions, S and W of Kangerlussuaq.		
600 Ma	Kimberlite intrusions S and W of Kangerlussuaq.		
100–50 Ma	Faulting related to sea-floor spreading during the opening of the Labrador Strait and Baffin Bay NNE-SSW sinistral strike slip faulting.	Probably the **Type 4** faults, the **Black** system.	
At least the last 2 Ma	Repeated glaciations resulting in erosion, glacier induced subsidence and rebound of the basement in the order of hundreds of meters + freeze thaw processes as deep as 400 meters may effect the stress fields and hence reactivate fractures and faults in the basement and hence effect the stress fields.		

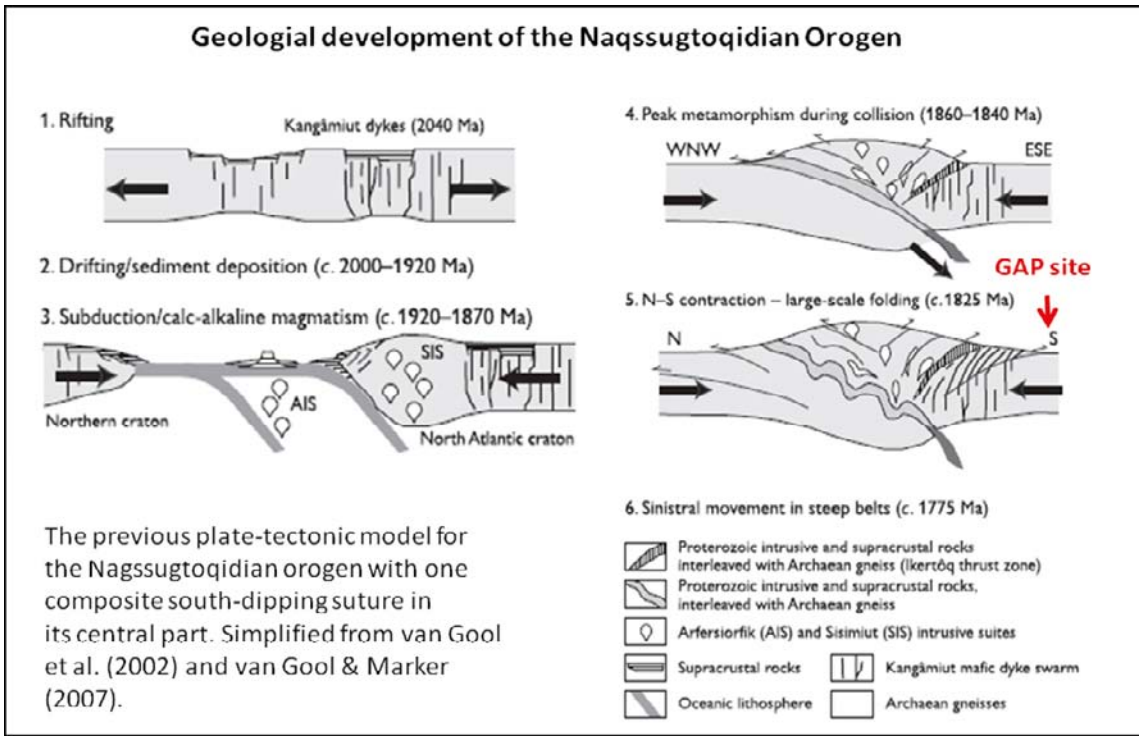

Figure 4-15. *Different tectonic stages during the development of the Naqssugtoqidian Orogen modified after Garde and Hollis (2010).*

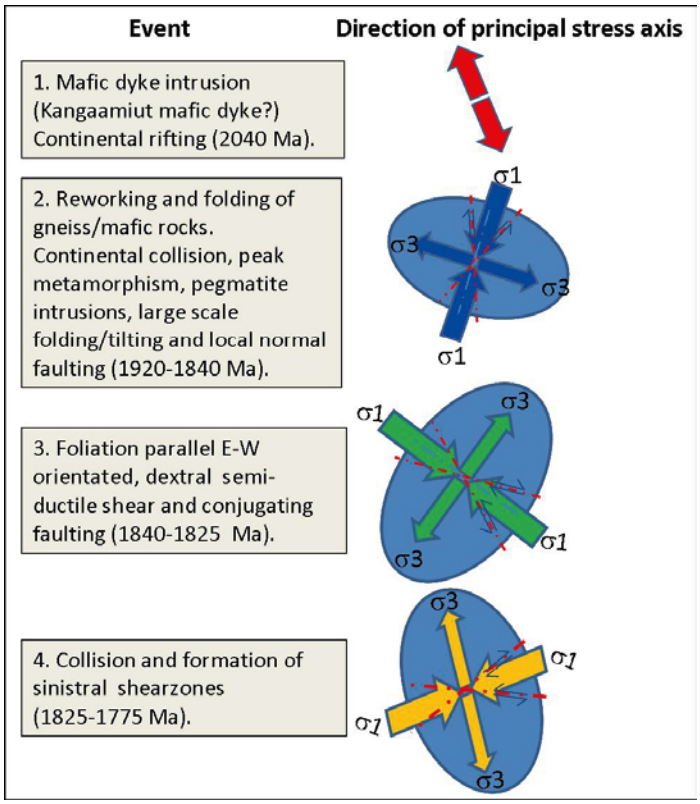

Figure 4-16. *Different tectonic stages and related stress fields during the development of the Naqssugtoqidian Orogen in the Kangerlussuaq area modified after Garde and Hollis (2010).*

Although the ancient stress fields in West Greenland are quite well known (Garde and Hollis 2010, Wilson et al. 2006, van Gool et al. 2002) and established the present day situation is more complex. According to Chung (2002) observation in Greenland shows a clear spatial correlation between seismicity and deglaciated areas along passive continental margins, which is evidence for earthquake triggering due to postglacial rebound. This support the theory that the shallow part of the lithosphere beneath the deglaciated margins in Greenland is under horizontal extension. The observed stress field can be explained as flexural stresses due to removal of ice loads and surface loads by glacial erosion. These local extensional stresses are further enhanced by the spreading stress of continental crust and reactivating of preexisting faults. Earthquake characteristics observed from Greenland suggest accordingly that the dominant seismogenic stresses are from postglacial rebound and spreading of the continental lithosphere. Finally, the presence of deep permafrost may also affect the stress field. The direction of the current stress field is of vital importance for modeling hydrological properties for the different Types of deformation zones/faults.

The dominant stresses in West Greenland seem to be of extensional nature enhanced by the spreading of the continental lithosphere following the ongoing opening of Baffin Bay when Canada and Greenland started to drift apart approximately 100 million years ago. At the western coast of Greenland the maximum horizontal stress trends NW-SE and the minimum horizontal stress trends NE-SW (Wilson et al. 2006). The presence of the Type 4 fault system, which is interpreted to be related to the opening of the Baffin Bay and Davies Strait, indicates prevailing stress conditions from this young tectonic event. However, the stress field at our site area might be somewhat different, because in this region the effects of the stress field from the old orogeny might still prevail.

5 Results and further work

The work of constraining a totally new 2-D model as an ArcGis map resulted in a deformation zone model that includes 158 zones (Figure 4-10). The data produced during the work, for GAP geological model version 1, is gathered in Appendix 2. The datasheet contains 10 different columns, where the most important ones are Type, Description, Location, Source, Dip and Orientation. Type refers to the four different types of zones described below. Description expresses the general trend of the zone while Location describes if it is located in our site area or in the regional area. Source explains from which sub-model the zone is derived from or if it is observed in both models. Column Dip and Orientation refers to dip in degrees and Orientation to direction of the dip for respective zones.

As stated above these deformation zones are interpreted to belong to four different types, which all can be identified both in site and regional scale. From the site scale data it is also evident that a fifth, sub-horizontal set of deformation exists, but due to the spatially limited data, its character and occurrence in a regional scale is difficult to estimate. The Type 5 set is therefore only mentioned briefly in the conclusions below and although its existence has been shown previously to be hydraulically important, its distribution is poorly constrained. The statistical variations in dip direction for Type 2 and Type 3 sets are estimated from their natural occurrence in the site area where data has been acquired (see Figure 4-11). The five different deformation zones/fault types are classified in Table 5-1 below.

The GAP geological model version 1 has refined and improved the geological understanding for both the site model and the regional model. Further work and mapping in the site area should be conducted to enhance the model and, especially the poorly constrained sub-horizontal Type 5 feature. Ideas and future actions to achieve this goal are listed below and tentatively it is planned that this work will be carried out during field season 2011.

Further work on the GAP geological model:

- Definition of the characteristics of deformation zones vs. lineaments.
- More detailed characterisation of the deformation zones and faults.
- Width and orientation for the different Types of deformation zones/faults.
- Compare our structural deformation history with studies done in other parts of Western Greenland, and couple these to the regional event stratigraphic interpretation.
- Characterisation of the bedrock (rock mass volume), comparison of fracture frequency in deformation zones and in between these zones.
- The modeled zones beneath the ice sheet should be compared against the radar data acquired on the ice sheet within Subproject A of the GAP project.

Even if the GAP geomodel version 1 produced a totally new 2-D model, further processing into 3-D was essential for the regional modelling area. Thus the data produced in this report was developed into a 3-D model that together with hydrological properties serves as basis for the future hydrological modelling within the GAP (Follin et al. 2011).

Table 5-1. Summary of the various Types of Deformation zones and Faults.

Type	Description of deformation zone	Orientation (Dip Direction)	Amount
Type 1 LILAC	Large scale deformation zones with both ductile and brittle features with roughly ENE-WSW orientation.	Dipping towards N, with steep to moderate dip 75°.	45
Type 2 GREEN	A smaller scale brittle deformation zone set, having a mainly a NW-SE orientation.	Steep to moderate dip 75°, towards NE (18 zones) and SW (6 zones).	24
Type 3 BLUE	Smaller scale brittle deformation zone set which is recognized as a system with mostly NE-SW orientation.	Moderate dip 70° towards SE (22 zones) and NW (21 zones).	43
Type 4 BLACK	An approximately NNE-SSW orientated fault system with a steep dip.	Vertical dip towards E or W.	46
Type 5 RED	A sub-horizontal deformation zone/fault set with shallow dip.	Sub-horizontal dip possibly towards SE, roughly 15°.	N/A

References

SKB's (Svensk Kärnbränslehantering AB) publications can be found at www.skb.se/publications.

Aaltonen I, Douglas B, Frape S, Henkemans E, Hobbs M, Klint K E, Lehtinen A, Claesson Liljendahl L, Lintinen P, Ruskeeniemi T, 2010. The Greenland Analouge Project, sub-project C, 2008 field and data report. Posiva Working Report 2010-62, Posiva Oy, Finland.

Chung W Y, 2002. Earthquakes along the passive margin of greenland: evidence for postglacial rebound control. Pure and Applied Geophysics 159, 2567–2584.

Escher A, 1971. Geologisk kort over Grønland 1:500.000, Kort nr. 3 Søndre Strømfjord–Nûssuaq.

Fairhead J D, Williams S E, 2006. Evaluating normalized magnetic derivatives for structural mapping. SEG Annual Meeting, New Orleans, Louisiana, 1–6 October 2006, Extended abstract.

Fairhead D, Williams S, Ben Salem A, 2007. Structural mapping from high resolution aeromagnetic data in namibia using normalized derivatives. EGM 2007 International Workshop: Innovation in EM, Grav and Mag Methods:a new Perspective for Exploration, Capri, Italy, 15–18 April 2007.

Follin S, Stigsson M, Rhén I, Engström J, Klint K E, 2011. Greenland Analogue Project – Hydraulic properties of deformation zones and fracture domains at Forsmark, Laxemar and Olkiluoto for usage together with geomodel version 1. SKB P-11-26, Svensk Kärnbränslehantering AB.

Garde A A, Hollis J A, 2010. A buried Paleoproterozoic spreading ridge in the northern Nagssugtoqidian orogen, West Greenland. Geological Society, London, Special Publications 338, 213–234.

Garde A A, Marker M, 2010. Geological map of Greenland, 1:500 000, Kangerlussuaq/Søndre Strømfjord–Nuussuaq, Sheet 3. 2nd ed. Copenhagen: Geological Survey of Denmark and Greenland.

Henkel H, Guzmán M, 1977. Magnetic features of fracture zones. Geoexploration 15, 173–181.

Jensen S M, Secher K, Rasmussen T M, Schjøth F, 2004. Diamond exploration data from West Greenland: 2004 update and revision. GEUS report 117, The Geological Survey of Denmark and Greenland.

Johnson H P, Merrill R T, 1972. Magnetic and mineralogical changes associated with low temperature oxidation of magnetite. Journal of Geophysical Research 77, 334–341.

Löfman J, Mészáros F, Keto V, Pitkänen P, Ahokas H, 2009. Modelling of groundwater flow and solute transport in Olkiluoto – Update 2008. Posiva Working Report 2009-78, Posiva Oy, Finland.

McIntyre J I, 1980. Geological significance of magnetic patterns related to magnetite in sediments and metasediments – a review. Bulletin of Australian Society of Exploration Geophysicists 11, 19–33.

Olofsson I, Simeonov A, Stephens M, Follin S, Nilsson A-C, Röshoff K, Lindberg U, Lanaro F, Fredriksson A, Persson L, 2007. Site descriptive modelling, Forsmark, stage 2.2. A fracture domain concept as a basis for the statistical modelling of fractures and minor deformation zones, and interdisciplinary coordination. SKB R-07-15, Svensk Kärnbränslehantering AB.

Phillips J D, 2007. Geosoft eXecutables (GX's) developed by the U.S. Geological Survey, version 2.0, with notes on GX development from Fortran code. Open-File Report 2007–1355, U.S. Geological Survey.

Salem A, Williams S, Fairhead D, Smith R, Ravat D, 2008. Interpretation of magnetic data using tilt-angle derivatives. Geophysics 73, L1–L10.

SKB, 2010. The Greenland Analogue Project. Yearly report 2009. SKB R-10-59, Svensk Kärnbränslehantering AB.

van Gool J A M, Connelly J N, Marker M, Mengel F C, 2002. The Nagssugtoqidian orogen of West Greenland: tectonic evolution and regional correlations from a West Greenland perspective. Canadian Journal of Earth Sciences 39, 665–686.

Wilson R W, Klint K E S, van Gool J A M, McCaffrey K J W, Holdsworth R E, Chalmers J A, 2006. Faults and fractures in central West Greenland: onshore expression of continental break-up and sea-floor spreading in the Labrador – Baffin Bay Sea. Geological Survey of Denmark and Greenland Bulletin 11, 185–204.

Appendix 1

Datasheet containing all lineaments in Sub-model 2, geophysical interpretation.

Lin_id	Data	Type	Length	Trend
geophys_0	magnetic tilt derivative	minimum	27,605	153
geophys_1	magnetic tilt derivative	minimum	16,442	21
geophys_2	magnetic tilt derivative	minimum	9,899	41
geophys_3	magnetic tilt derivative	minimum	14,380	25
geophys_4	magnetic tilt derivative	minimum	12,895	7
geophys_5	magnetic tilt derivative	minimum	6,611	14
geophys_6	magnetic tilt derivative	minimum	4,756	16
geophys_7	magnetic tilt derivative	minimum	4,881	8
geophys_8	magnetic tilt derivative	minimum	36,045	64
geophys_9	magnetic tilt derivative	minimum	62,227	81
geophys_10	magnetic tilt derivative	minimum	46,086	66
geophys_11	magnetic tilt derivative	minimum	26,418	95
geophys_12	magnetic tilt derivative	minimum	11,384	54
geophys_13	magnetic tilt derivative	minimum	21,027	75
geophys_14	magnetic tilt derivative	minimum	85,911	75
geophys_15	magnetic tilt derivative	minimum	25,444	69
geophys_16	magnetic tilt derivative	minimum	18,912	66
geophys_17	magnetic tilt derivative	minimum	20,775	57
geophys_18	magnetic tilt derivative	minimum	24,430	55
geophys_19	magnetic tilt derivative	minimum	56,297	77
geophys_20	magnetic tilt derivative	minimum	10,299	90
geophys_21	magnetic tilt derivative	minimum	11,835	83
geophys_22	magnetic total field	minimum	65,259	76
geophys_23	magnetic total field	minimum	25,120	122
geophys_24	magnetic total field	minimum	15,579	12
geophys_25	magnetic total field	minimum	9,189	41
geophys_26	magnetic total field	minimum	11,722	137
geophys_27	magnetic total field	minimum	19,547	117
geophys_28	magnetic total field	minimum	18,486	63
geophys_29	magnetic total field	minimum	67,692	72
geophys_30	magnetic total field	minimum	23,767	61
geophys_31	magnetic total field	minimum	9,969	111
geophys_32	magnetic total field	minimum	13,639	110
geophys_33	magnetic total field	minimum	18,052	79
geophys_34	magnetic total field	minimum	11,334	64
geophys_35	magnetic total field	minimum	14,891	52
geophys_36	magnetic total field	minimum	12,936	44
geophys_37	magnetic total field	minimum	16,941	58
geophys_38	magnetic total field	minimum	22,125	129
geophys_39	magnetic total field	minimum	16,113	59
geophys_40	magnetic total field	minimum	16,551	49
geophys_41	magnetic tilt derivative	minimum	6,523	161
geophys_42	magnetic tilt derivative	minimum	19,267	44
geophys_43	magnetic tilt derivative	minimum	19,949	41
geophys_44	magnetic tilt derivative	minimum	4,136	23
geophys_45	magnetic tilt derivative	minimum	29,747	71
geophys_46	magnetic tilt derivative	minimum	29,401	72
geophys_47	magnetic tilt derivative	minimum	6,765	76
geophys_48	magnetic tilt derivative	minimum	12,517	69
geophys_49	magnetic tilt derivative	minimum	20,965	67
geophys_50	magnetic tilt derivative	minimum	20,839	43
geophys_51	magnetic total field	minimum	6,251	6

Lin_id	Data	Type	Length	Trend
geophys_52	magnetic total field	minimum	30,785	79
geophys_53	magnetic total field	minimum	18,210	67
geophys_54	magnetic total field	minimum	24,836	65
geophys_55	magnetic total field	minimum	5,057	65
geophys_56	magnetic total field	minimum	7,255	63
geophys_57	magnetic vertical derivative	minimum	9,818	80
geophys_58	magnetic vertical derivative	minimum	22,365	66
geophys_59	magnetic vertical derivative	minimum	20,870	57
geophys_60	magnetic vertical derivative	minimum	19,255	57
geophys_61	magnetic vertical derivative	minimum	14,090	87
geophys_62	magnetic vertical derivative	minimum	8,473	79
geophys_63	magnetic vertical derivative	minimum	6,100	65
geophys_64	magnetic vertical derivative	minimum	10,965	60
geophys_65	magnetic vertical derivative	minimum	20,852	63
geophys_66	magnetic vertical derivative	minimum	56,785	67
geophys_67	magnetic vertical derivative	minimum	6,225	46
geophys_68	magnetic vertical derivative	minimum	5,635	27
geophys_69	magnetic vertical derivative	minimum	29,978	84
geophys_70	magnetic vertical derivative	minimum	32,222	78
geophys_71	magnetic vertical derivative	minimum	33,989	60
geophys_72	magnetic tdx derivative	maximum	11,262	44
geophys_73	magnetic tdx derivative	maximum	5,864	33
geophys_74	magnetic tdx derivative	maximum	2,868	21
geophys_75	magnetic total field	minimum	5,938	8
geophys_76	magnetic total field	minimum	19,299	79
geophys_77	magnetic total field	minimum	22,538	80
geophys_78	magnetic vertical derivative	minimum	9,105	141
geophys_79	magnetic vertical derivative	minimum	7,941	138
geophys_80	magnetic tilt derivative	minimum	32,966	74
geophys_81	magnetic tilt derivative	minimum	3,762	63
geophys_82	magnetic tilt derivative	minimum	4,819	49
geophys_83	magnetic tilt derivative	minimum	4,290	34
geophys_84	magnetic tilt derivative	minimum	2,721	28
geophys_85	magnetic tilt derivative	minimum	4,738	46
geophys_86	magnetic tilt derivative	minimum	12,959	94
geophys_87	magnetic tilt derivative	minimum	23,161	71
geophys_88	magnetic tilt derivative	minimum	11,210	72
geophys_89	magnetic tilt derivative	minimum	5,000	14
geophys_90	magnetic total field	minimum	4,049	4
geophys_91	magnetic total field	minimum	5,267	139
geophys_92	magnetic total field	minimum	14,544	70
geophys_93	magnetic total field	minimum	8,697	73
geophys_94	magnetic tilt derivative	minimum	42,191	71
geophys_95	magnetic tilt derivative	minimum	6,414	11
geophys_96	magnetic tilt derivative	minimum	15,540	87
geophys_97	magnetic total field	minimum	5,269	58
geophys_98	magnetic tilt derivative	minimum	7,822	27
geophys_99	magnetic tilt derivative	minimum	5,867	35
geophys_100	magnetic tilt derivative	minimum	4,633	55
geophys_101	magnetic tilt derivative	minimum	6,264	52
geophys_102	magnetic tilt derivative	minimum	4,645	34
geophys_103	magnetic tilt derivative	minimum	3,883	148
geophys_104	magnetic tilt derivative	minimum	8,925	107
geophys_105	magnetic tilt derivative	minimum	2,120	16
geophys_106	magnetic tilt derivative	minimum	3,180	9
geophys_107	magnetic tilt derivative	minimum	5,086	80

Lin_id	Data	Type	Length	Trend
geophys_108	magnetic tilt derivative	minimum	12,178	80
geophys_109	magnetic tilt derivative	minimum	4,350	62
geophys_110	magnetic tilt derivative	minimum	5,448	77
geophys_111	magnetic tilt derivative	minimum	10,094	88
geophys_112	magnetic tilt derivative	minimum	7,279	54
geophys_113	magnetic tilt derivative	minimum	5,254	27
geophys_114	magnetic tilt derivative	minimum	5,664	46
geophys_115	magnetic tilt derivative	minimum	2,580	164
geophys_116	magnetic tilt derivative	minimum	1,916	166
geophys_117	magnetic tilt derivative	minimum	2,276	173
geophys_118	magnetic tilt derivative	minimum	5,655	61
geophys_119	magnetic tilt derivative	minimum	6,307	71
geophys_120	magnetic tilt derivative	minimum	11,596	35
geophys_121	magnetic tilt derivative	minimum	5,668	171
geophys_122	magnetic tilt derivative	minimum	18,407	69
geophys_123	magnetic tilt derivative	minimum	20,434	133
geophys_124	magnetic tilt derivative	minimum	7,655	155
geophys_125	magnetic tilt derivative	minimum	10,008	168
geophys_126	magnetic tilt derivative	minimum	9,744	81
geophys_127	magnetic tilt derivative	minimum	8,870	80
geophys_128	magnetic horizontal derivative	minimum	11,415	91
geophys_129	magnetic horizontal derivative	minimum	3,302	14
geophys_130	magnetic horizontal derivative	minimum	17,631	127
geophys_131	magnetic horizontal derivative	minimum	11,264	37
geophys_132	magnetic total field	minimum	15,897	62

Appendix 2

Datasheet containing all deformation zones in GAP geological version 1.

Object_id	Shape	Type	Numbers	Description	Location	Shape_length	Source	Dip	Orientation
1		1	1	WSW-ENE	Site	45,742.26	Geo+GP	75	N
2		1	2	WSW-ENE	Regional	83,486.61	Geo+GP	75	N
3		1	3	WSW-ENE	Regional	110,950.3	Geo+GP	75	N
4		1	4	WSW-ENE	Regional	41,314.96	Geo+GP	75	N
5		1	5	W-E	Site	60,334.18	Geo+GP	75	N
6		1	6	WSW-ENE	Regional	33,152.58	Geo	75	N
7		1	7	WSW-ENE	Regional	28,520.7	Geo	75	N
8		1	8	WSW-ENE	Regional	41,023.32	Geo+GP	75	N
9		1	9	WSW-ENE	Regional	52,391.73	Geo+GP	75	N
10		1	10	WSW-ENE	Regional	26,680.69	Geo+GP	75	N
11		1	11	WSW-ENE	Regional	68,997.6	Geo+GP	75	N
12		1	12	WSW-ENE	Regional	32,142.5	Geo+GP	75	N
13		1	13	WSW-ENE	Regional	113,470.5	Geo+GP	75	N
14		1	14	WSW-ENE	Regional	64,896.72	Geo+GP	75	N
15		1	15	W-E	Regional	17,055.56	Geo+GP	75	N
16		1	16	W-E	Regional	20,797.71	Geo	75	N
17		1	17	W-E	Regional	8,782.322	Geo+GP	75	N
18		1	18	W-E	Regional	13,504.97	Geo	75	N
19		1	19	W-E	Site	7,609.631	Geo	75	N
20		1	20	WSW-ENE	Regional	15,314.08	GP	75	N
83		1	65	WSW-ENE	Regional	61,592.58	Geo+GP	75	N
105		1	105	WSW-ENE	Regional	25,688.96	GP	75	N
106		1	106	WSW-ENE	Regional	27,491.39	GP	75	N
107		1	107	WSW-ENE	Regional	14,024.32	GP	75	N
108		1	108	WSW-ENE	Regional	13,388.62	GP	75	N
109		1	109	WSW-ENE	Regional	66,045.66	GP	75	N
111		1	111	WSW-ENE	Regional	51,476.67	GP	75	N
113		1	113	W-E	Regional	31,298.33	GP	75	N
116		1	116	W-E	Regional	16,675.3	GP	75	N
119		1	119	WSW-ENE	Regional	25,314.23	GP	75	N
120		1	120	WSW-ENE	Regional	34,037.24	GP	75	N
121		1	121	WSW-ENE	Regional	24,066.75	GP	75	N
123		1	123	W-E	Regional	23,809.04	GP	75	N
124		1	124	WSW-ENE	Regional	11,962	GP	75	N
128		1	128	WSW-ENE	Regional	57,843.91	GP	75	N
129		1	129	WSW-ENE	Regional	21,140.45	Geo+GP	75	N
130		1	130	WSW-ENE	Regional	22,726.05	GP	75	N
131		1	131	WSW-ENE	Regional	27,537.59	GP	75	N
132		1	132	WSW-ENE	Regional	24,191.54	GP	75	N
133		1	133	WSW-ENE	Regional	22,621.56	Geo+GP	75	N
141		1	141	W-E	Regional	23,337	GP	75	N
142		1	142	W-E	Regional	51,464.79	GP	75	N
150		1	150	WSW-ENE	Regional	22,859.78	GP	75	N
154		1	154	WSW-ENE	Regional	16,261.2	GP	75	N
157		1	157	WSW-ENE	Regional	43,716.89	GP	75	N
21		2	21	NW-SE	Regional	50,903.73	Geo+GP	75	NE
22		2	22	NW-SE	Regional	19,572.8	Geo+GP	75	SW
23		2	23	WNW-ESE	Regional	8,331.7	Geo	75	NE
24		2	24	NW-SE	Site	9,709.805	Geo+GP	75	NE
25		2	25	NW-SE	Regional	8,932.379	Geo	75	NE
26		2	26	WNW-ESE	Site	1,590.375	Geo	75	NE
27		2	27	NW-SE	Site	5,973.128	Geo	75	NE

Object_id	Shape	Type	Numbers	Description	Location	Shape_length	Source	Dip	Orientation
28		2	28	NW-SE	Regional	7,837.726	Geo	75	NE
29		2	29	NW-SE	Regional	5,179.617	Geo	75	NE
30		2	30	WNW-ESE	Regional	19,227.68	Geo	75	NE
31		2	31	WNW-ESE	Regional	7,382.585	Geo	75	SW
32		2	32	NW-SE	Regional	20,218.91	Geo	75	NE
33		2	33	NW-SE	Regional	11,885.22	Geo+GP	75	NE
34		2	34	NW-SE	Regional	18,056.77	Geo	75	NE
114		2	114	NW-SE	Regional	21,789.48	GP	75	NE
117		2	117	WNW-ESE	Regional	24,520.75	GP	75	SW
125		2	125	NW-SE	Regional	5,377.963	GP	75	NE
134		2	134	NW-SE	Regional	9,798.465	GP	75	SW
135		2	135	NW-SE	Regional	7,807.733	GP	75	NE
136		2	136	NW-SE	Regional	6,602.058	GP	75	NE
146		2	146	NW-SE	Regional	17,866.94	GP	75	NE
147		2	147	WNW-ESE	Regional	29,303.18	GP	75	SW
148		2	148	WNW-ESE	Regional	24,974.68	GP	75	NE
149		2	149	NW-SE	Regional	5,022.912	GP	75	SW
35		3	35	SW-NE	Regional	19,304.08	GP	70	NW
36		3	36	SW-NE	Regional	19,841.11	Geo+GP	70	NW
37		3	37	SW-NE	Regional	19,081.27	Geo	70	NW
38		3	38	SW-NE	Regional	5,376.239	Geo	70	NW
39		3	39	SW-NE	Regional	15,798.15	Geo	70	NW
40		3	40	SW-NE	Regional	8,474.957	Geo	70	NW
41		3	41	SW-NE	Regional	17,293.67	Geo+GP	70	NW
42		3	42	SW-NE	Regional	14,003.14	Geo+GP	70	NW
43		3	43	SW-NE	Site	7,848.332	Geo+GP	70	SE
44		3	44	SW-NE	Site	25,229.1	Geo+GP	70	NW
45		3	45	SW-NE	Site	10,231.48	Geo+GP	70	SE
46		3	46	SW-NE	Site	2,720.348	Geo	70	SE
47		3	47	SW-NE	Site	8,037.779	Geo+GP	70	SE
48		3	48	SW-NE	Site	14,223.04	Geo+GP	70	NW
49		3	49	SW-NE	Regional	25,514.74	Geo+GP	70	SE
50		3	50	SW-NE	Regional	14,905.82	Geo	70	SE
51		3	51	SW-NE	Regional	14,391.73	Geo	70	NW
52		3	52	SW-NE	Regional	18,375.48	Geo	70	NW
53		3	53	SW-NE	Regional	13,180.11	Geo	70	NW
54		3	54	SW-NE	Regional	30,433.07	Geo+GP	70	SE
55		3	55	SW-NE	Regional	33,848.58	Geo+GP	70	SE
56		3	56	SW-NE	Regional	35,748.22	Geo+GP	70	SE
57		3	57	SW-NE	Regional	13,465.03	Geo+GP	70	NW
58		3	58	SW-NE	Regional	20,482.72	Geo+GP	70	NW
59		3	59	SW-NE	Regional	20,199.1	Geo+GP	70	NW
60		3	60	SW-NE	Regional	28,138.54	Geo+GP	70	SE
75		3	62	SW-NE	Regional	17,197.23	Geo	70	SE
79		3	63	SW-NE	Regional	22,610.81	Geo+GP	70	SE
85		3	67	SW-NE	Regional	23,927.55	Geo+GP	70	SE
86		3	68	SW-NE	Regional	4,813.633	Geo	70	SE
89		3	70	SW-NE	Regional	14,672.7	Geo	70	SE
73		3	71	SW-NE	Site	11,419.13	Geo+GP	70	SE
74		3	104	SW-NE	Site	3,765.283	Geo	70	NW
122		3	122	SW-NE	Regional	11,125.24	GP	70	SE
137		3	137	SW-NE	Regional	11,111.4	GP	70	SE
138		3	138	SW-NE	Regional	4,625.846	GP	70	SE
143		3	143	SW-NE	Regional	7,851.364	GP	70	SE
144		3	144	SW-NE	Regional	11,668.46	GP	70	NW
145		3	145	SW-NE	Regional	8,033.832	GP	70	SE

Object_id	Shape	Type	Numbers	Description	Location	Shape_length	Source	Dip	Orientation
151		3	151	SW-NE	Regional	9,192.178	GP	70	SE
152		3	152	SW-NE	Regional	14,799.38	GP	70	NW
153		3	153	SW-NE	Regional	12,975.33	GP	70	NW
158		3	158	SW-NE	Regional	6,221.267	GP	70	NW
61		4	61	SSW-NNE	Regional	25,904.32	Geo+GP	90	E or W
80		4	64	SSW-NNE	Regional	35,657.52	Geo+GP	90	E or W
84		4	66	SSW-NNE	Regional	11,128.28	Geo	90	E or W
88		4	69	SSW-NNE	Regional	6,207.281	Geo+GP	90	E or W
76		4	72	SSW-NNE	Regional	24,793.55	Geo	90	E or W
87		4	73	SSW-NNE	Regional	21,302.79	Geo+GP	90	E or W
77		4	74	SSW-NNE	Regional	12,656.3	Geo	90	E or W
78		4	75	SSW-NNE	Regional	7,536.356	Geo	90	E or W
81		4	76	SSW-NNE	Regional	7,583.114	Geo	90	E or W
82		4	77	SSW-NNE	Regional	6,257.367	Geo	90	E or W
91		4	78	SSW-NNE	Regional	14,094.62	Geo	90	E or W
92		4	79	SSW-NNE	Regional	19,789.07	Geo+GP	90	E or W
93		4	80	SSW-NNE	Regional	8,920.258	Geo	90	E or W
94		4	81	SSW-NNE	Regional	3,118.658	Geo	90	E or W
95		4	82	SSW-NNE	Regional	12,975.47	Geo	90	E or W
96		4	83	SSW-NNE	Regional	10,999.62	Geo	90	E or W
97		4	84	SSW-NNE	Regional	14,340.06	Geo	90	E or W
98		4	85	SSW-NNE	Regional	12,972.31	Geo	90	E or W
99		4	86	SSW-NNE	Regional	49,652.82	Geo+GP	90	E or W
100		4	87	SSW-NNE	Regional	23,772.19	Geo+GP	90	E or W
101		4	88	SSW-NNE	Regional	14,758.49	Geo+GP	90	E or W
102		4	89	SSW-NNE	Regional	22,718.55	Geo+GP	90	E or W
103		4	90	SSW-NNE	Regional	15,364.52	Geo	90	E or W
104		4	91	SSW-NNE	Regional	17,478.12	Geo+GP	90	E or W
62		4	92	SSW-NNE	Regional	12,105.93	Geo	90	E or W
63		4	93	N-S	Regional	5,180.211	Geo	90	E or W
64		4	94	SSW-NNE	Regional	9,921.862	Geo	90	E or W
67		4	95	N-S	Regional	5,512.338	Geo	90	E or W
65		4	96	N-S	Regional	17,865.44	Geo+GP	90	E or W
66		4	97	N-S	Regional	15,912.86	Geo	90	E or W
68		4	98	SSW-NNE	Regional	14,594.93	Geo	90	E or W
69		4	99	SSW-NNE	Regional	9,114.393	Geo	90	E or W
71		4	100	NNW-SSE	Site	7,777.038	Geo+GP	90	E or W
70		4	101	SSW-NNE	Regional	13,946.42	Geo	90	E or W
72		4	102	N-S	Site	3,258.364	Geo	90	E or W
90		4	103	SSW-NNE	Regional	9,167.126	Geo	90	E or W
110		4	110	SSW-NNE	Regional	9,986	Geo+GP	90	E or W
112		4	112	SSW-NNE	Regional	5,489.731	Geo	90	E or W
115		4	115	SSW-NNE	Regional	4,997.441	Geo+GP	90	E or W
118		4	118	NNW-SSE	Regional	10,096.3	GP	90	E or W
126		4	126	N-S	Regional	3,130.851	GP	90	E or W
127		4	127	SSW-NNE	Site	3,252.638	GP	90	E or W
139		4	139	SSW-NNE	Regional	3,814.435	GP	90	E or W
140		4	140	SSW-NNE	Regional	4,208.531	GP	90	E or W
155		4	155	NNW-SSE	Regional	7,359.374	GP	90	E or W
156		4	156	N-S	Site	2,638.526	GP	90	E or W